ACI STRUCTURAL JOURNAL TECHNICAL PAPER

Title No. 114-S19

Behavior of Monotonically Loaded Slab-Column Connections Reinforced with Shear Studs

by Thai X. Dam, James K. Wight, and Gustavo J. Parra-Montesinos

A total of five full-scale interior slab-column connections were tested under concentric monotonically increased loading. The slabs were 10 ft (3050 mm) square and 10 in. (254 mm) thick, and columns were 12 x 12 in. (305 x 305 mm). The specimens were built with Grade 60 reinforcement and 4000 psi (27.6 MPa) normal-weight concrete. Slab flexural tension reinforcement ratios were 0.87% in three specimens and 1.25% in the other two. One specimen with a slab reinforcement ratio of 0.87% was built without shear reinforcement. The other specimens were reinforced with headed shear studs. The studs were placed in either a radial or an orthogonal layout. Test results show that shear strength equations in the ACI Building Code overestimated the strength of the slab-column connections with a 0.87% slab flexural reinforcement ratio. Also, significant differences in failure mode were observed between slab-column connections with shear studs arranged in a radial layout and those with an orthogonal stud arrangement. Recommendations to improve shear strength of slab-column connections are presented.

Keywords: punching shear; shear reinforcement layout; shear studs; two-way slab.

INTRODUCTION

Headed shear studs are a popular form of shear reinforcement used in two-way floor systems at slab-column connections, where either concentric shear or shear and moment are transferred from the slab to the column.[1-3] Shear studs are often welded to a steel plate to form an assembly normally referred to as a stud rail.[4,5] In North America, stud rails are typically placed perpendicular to column faces in a so-called orthogonal (or cruciform) layout (Fig. 1(a)) to reduce interferences with slab flexural reinforcement. A potential issue with this layout of shear studs is that large regions of the slab extending out from the corners of the columns are essentially unreinforced in shear. This issue can be addressed by placing stud rails that project radially out from the corners of the column, referred to herein as a radial layout (Fig. 1(b)). Some research investigations[6-9] have indicated that stud layout (radial versus orthogonal) has no effect on shear strength of slab-column connections. However, other research investigations[10-12] have indicated that there may be a significant difference in behavior and shear strength of slab-column connections with a radial versus an orthogonal layout of shear studs. A reason for these apparently conflicting research results may be related to the percentage of flexural reinforcement in the slab near the slab-column connection.

The research presented herein was aimed at experimentally studying the behavior of large-scale slab-column connections under concentric gravity loading, with a focus on the effect of: 1) the layout of stud rails; and 2) the percentage of slab flexural reinforcement on the behavior and shear strength of slab-column connections.

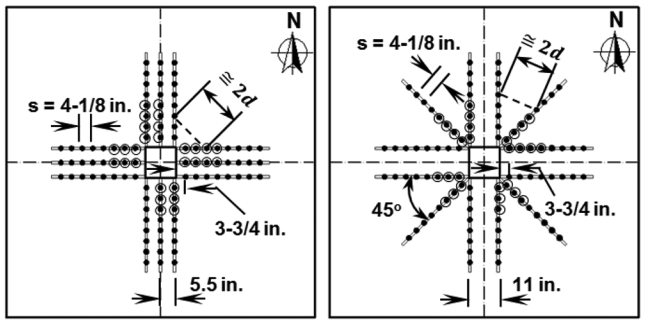

(Note: ○ studs with strain gauges, 1 in. = 25.4 mm)
a) Orthogonal layout (S08O & S12O) b) radial layout (S08R & S12R)

Fig. 1—Shear stud layouts and strain gauge locations (circles).

Notation—For the sake of convenience, the term "slab shear stress" in this paper, shown as v, refers to the average shear stress calcualted at a critical section located a distance $d/2$ (d is the average effective depth of a slab) away from the column faces, as defined in the ACI Building Code.[13] If V is the shear force transferred between the slab and column, and b_o is the perimeter of the critical section, slab shear stress $v = V/b_o d$.

RESEARCH SIGNIFICANCE

Results from tests of five full-scale reinforced concrete slab-column connections under concentric monotonically increased loading are presented. Results from these tests allow a better understanding of the effect of the percentage of slab flexural reinforcement and the layout of shear studs on behavior and shear strength of reinforced concrete slab-column connections subjected to gravity loading. Recommendations to improve shear strength of slab-column connections are presented.

RESEARCH MOTIVATION

DaCosta and Parra-Montesinos[11] tested several slab-column connections to evaluate the effect of shear stud

ACI Structural Journal, V. 114, No. 1, January-February 2017.
MS No. S-2016-066, doi: 10.14359/51689165, received February 5, 2016, and reviewed under Institute publication policies.

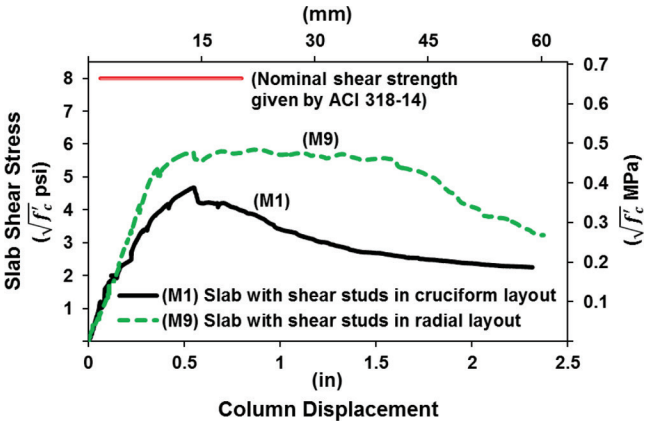

Fig. 2—Results from DaCosta and Parra-Montesinos[11] tests.

layout on the behavior of slab-column connections under simulated gravity load. The behavior of two connections, M1 and M9, is discussed herein. Aside from the configuration of shear studs, the two test specimens were nominally identical. Slabs of the test specimens were 6 x 6 ft (1830 x 1830 mm) and 8 in. (200 mm) thick. These were loaded concentrically through a 6 x 6 in. (150 x 150 mm) square column. The slabs had an average flexural tension reinforcement ratio ρ of approximately 0.80%, and an effective depth *d* of approximately 6.5 in. (165 mm). The slabs in Specimens M1 and M9 were reinforced by eight identical stud rails using layouts similar to those in Fig. 1(a) and 1(b), respectively. Each stud rail contained 12 shear studs with a shaft diameter of 3/8 in. (9.5 mm) at a spacing of 3*d*/8, or 2.5 in (65 mm). The first peripheral line of shear studs was at approximately 2 in. (50 mm) from the column faces.

Relationships between measured slab shear stress and column displacement for the two connections are plotted in Fig. 2. Test results indicated that: 1) the two specimens failed due to punching shear at a load significantly lower than the design shear strength given by the ACI Code[13]; 2) shear studs configured in the cruciform layout were substantially less effective than those placed in a radial layout in terms of shear strength and ductility; and 3) Specimen M9 experienced significant yielding of slab flexural reinforcement before the punching failure occurred. The results reported by DaCosta and Parra-Montesinos raised concerns regarding the safety of slab-column connections with a low slab flexural reinforcement ratio and an orthogonal layout of stud rails.

EXPERIMENTAL PROGRAM

Overall specimen configuration

All of the slab-column connections in this study had the same geometry. These represented interior slab-column connections from a reinforced concrete flat plate structure with 10 in. (254 mm) thick slabs supported by 12 x 12 in. columns (305 x 305 mm) approximately 25 ft (7620 mm) apart. Slabs in the test specimens were 10 x 10 ft (3050 x 3050 mm), with a column located at the center of the slab (Fig. 3(a)). The specimens were supported at eight different locations around the slab perimeter and tested upside-down for testing convenience.

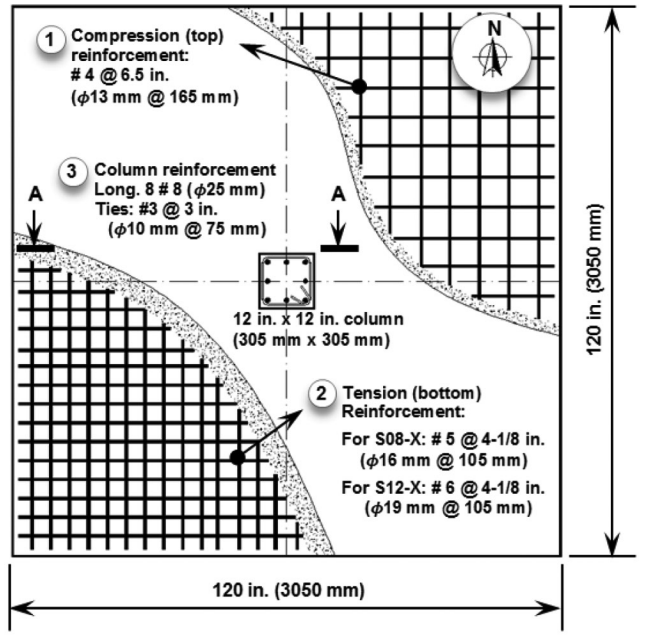

a) Top view

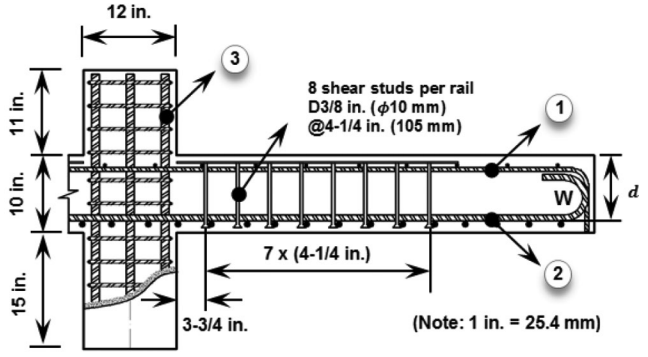

b) Section A-A (Fig. 3a)

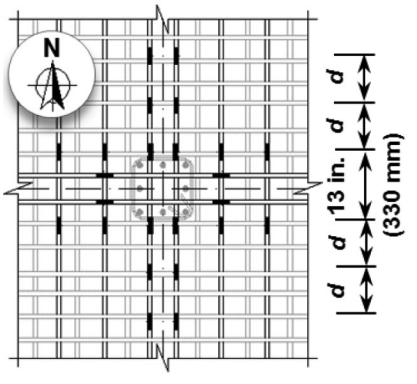

c) Strain gauge locations (▬) in slab tension (bottom) reinforcement

Fig. 3—Flexural and shear reinforcement details.

The primary parameters for the tests were the average slab flexural reinforcement ratio ρ and shear stud layout. Three specimens had ρ = 0.87%, labeled as S08C, S08O, and S08R, and the other two specimens had a higher ρ =

1.25%, labeled as S12O and S12R. In these specimen labels, the letter S stood for "Specimen", and the numbers 08 and 12 represented the approximate slab flexural reinforcement ratio (0.87 and 1.25%). Specimen S08C was built without shear reinforcement and served as a Control specimen. The remaining four specimens were reinforced with the same number of shear studs configured in two different layouts. For Specimens S08O and S12O, stud rails were placed in an Othogonal layout (Fig. 1(a)), and for Specimens S08R and S12R, the stud rails were arranged in a Radial layout (Fig. 1(b)).

Specimen design

It was assumed that the resultant of the forces acting on the specimens passed through the center of the slabs and, thus, no moments were transferred from the slabs to the columns. Flexural reinforcement was Grade 60, and the specified concrete compressive strength was 4000 psi (27.6 MPa).

Flexural reinforcement—Slab flexural tension reinforcement consisted of No. 5 bars (ϕ16 mm) for the S08 specimens and No. 6 bars (ϕ19 mm) for the S12 specimens, spaced at 4-1/8 in. (105 mm). The average effective depth d was 8.63 and 8.5 in. (220 and 215 mm) for the S08 and S12 specimens, respectively. The average percentage of slab flexural reinforcement was 0.87% for the S08 specimens and 1.25% for the S12 specimens. Because the specimens were tested upside-down, the primary flexural reinforcement was placed at the bottom of the slabs. The compression (top) reinforcement in the slabs consisted of No. 4 bars (ϕ13 mm) at a spacing of 6.5 in. (165 mm), with two bars passing through the column core to satisfy the structural integrity requirement in the ACI Code[13] and reflect general construction practice. The bars for the top and bottom layers were placed symmetrically about the center of the slabs (Fig. 3(b)). The column longitudinal reinforcement consisted of eight No. 8 bars, which were equally distributed around the column core. Ties were No. 3 bars (ϕ10 mm) at a spacing of 3 in. (75 mm) along the entire column length (Fig. 3(b)).

Shear reinforcement—Specimen S08C was built without shear reinforcement. Its nominal shear strength, as given by the ACI Code,[13] was $V_{shear} = 4\sqrt{f_c'}b_o d$ lb ($0.33\sqrt{f_c'}b_o d$ kN). The other specimens were reinforced with the same amount of shear reinforcement and their nominal shear strength, as given by the ACI Code,[13] can be computed from Eq. (1),

$$V_{shear} = (v_c + v_s)b_o d \quad (1)$$

where v_c and v_s are shear strength, expressed as a stress, provided by the concrete and shear reinforcement, respectively. Shear reinforcement was designed so that $v_c + v_s \cong 6\sqrt{f_c'}$ psi ($0.5\sqrt{f_c'}$ MPa). Twelve identical stud rails,[14] manufactured in accordance with ASTM A1044/A1044M,[15] were used in each shear-reinforced specimen. For each stud rail, eight shear studs were welded symmetrically to a 36 in. (915 mm) long rail at a uniform spacing of 4-1/8 in. (105 mm). The shaft diameter of the studs was 3/8 in. (10 mm), and the rail width and thickness were 1 and 3/16 in. (25.4 and 4.8 mm), respectively. The total height of the stud rails was 8.5 in. (215 mm) to satisfy the requirements in the ACI Code.[13] The stud rails were arranged in an orthogonal layout (Fig. 1(a)) for Specimens S08O and S12O, and in a radial layout (Fig. 1(b)) for Specimens S08R and S12R. For the latter specimens, the fourth slab flexural tension reinforcing bars (bottom) from the center of the slabs were adjusted approximately 3/4 in. (18 mm) toward the edges of the slabs to place the diagonal stud rails. The first studs were located at 3.75 in. (95 mm) away from the column faces or corners. The maximum peripheral spacing was smaller than 2d for the first three rows of shear studs in an orthogonal layout, and for the first five rows in a radial layout (Fig. 1). A summary of design details for all test specimens is given in Table 1.

Table 1—Specimens information and measured material properties

Specimen ID	Slab flexural reinforcement ratio ρ, %	Shear stud layout	f_c', psi (MPa)	f_y, ksi (MPa)	V_{shear}, kip (kN)
(1)	(2)	(3)	(4)	(4)	(5)
S08C	0.87	—	6100 (42.1)	66.5 (460)	222 (990)
S08O	0.87	Ortho.	5050 (34.8)	66.5 (460)	317 (1410)
S08R	0.87	Radial	5360 (37.0)	66.5 (460)	322 (1430)
S12O	1.25	Ortho.	4510 (31.1)	65.0 (450)	304 (1350)
S12R	1.25	Radial	4790 (33.0)	65.0 (450)	308 (1370)

Notes: Measured yield strength of shear studs; f_{yt} = 71.1 ksi (490 MPa).

Material properties

Concrete—All specimens were cast in two phases with normalweight concrete. The slab and the bottom column stub were cast first using ready mixed concrete, and then the top column stub was cast a few days later using concrete mixed in the laboratory. One concrete mixture design was used throughout the project to assure consistency for the concrete used in the five specimens. The concrete was specified to have a 28-day compressive strength of 4000 psi (27.6 MPa), a slump of 6 in. (150 mm), and a maximum aggregate size of 1/2 in. (13 mm). The mixture proportions by weight of cement, fly ash, water, sand, and coarse aggregate were 1:0.37:0.74:5.05:5.35, respectively. The compressive strengths of the slab concrete, f_c', for all specimens, measured through 4 x 8 in. (100 x 200 mm) cylinders on the day of testing, are given in Table 1.

Reinforcement—Measured yield strength of flexural reinforcement, f_y, was 65,000, 66,500, and 60,000 psi (450, 460, and 415 MPa) for No. 6, No. 5, and No. 4 reinforcing bars, respectively. For the shear studs, the measured yield strength was 71,100 psi (490 MPa), but the upper limit of 60,000 psi (415 MPa) was used to calculate the ACI Code[13] nominal shear strength (V_{shear}).

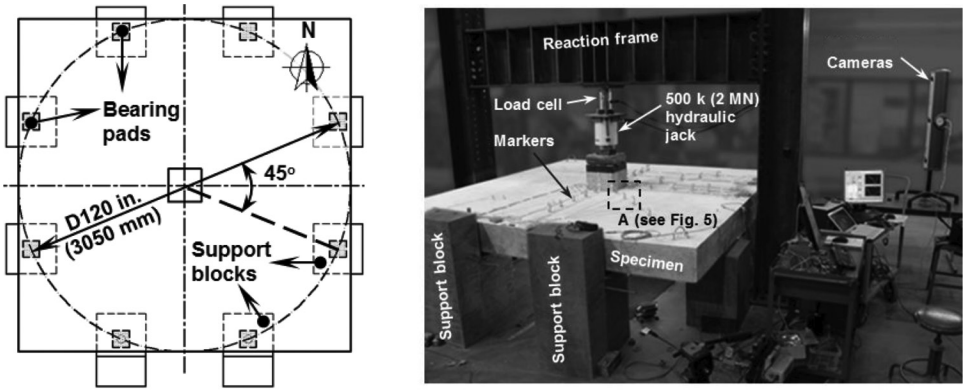

a) Support systems b) Apparatus

Fig. 4—Test setup.

Test setup

Support system—The slabs were supported by eight reinforced concrete blocks that were placed in a symmetrical pattern around the center of the slab (Fig. 4(a)). The supporting system was intended to simulate the contraflexural line, approximately a circle with a diameter of 10 ft (3050 mm). Neoprene bearing pads and thin steel plates were used at every supporting point to create a level support surface between the blocks and the slab. The neoprene pads were used to distribute loads equally from the slab to the supports and to provide free rotation and negligible in-plane restraint at the edge of the slabs.

Loading method—A vertical downward force was applied at the top of the column by a 500 kip (2.2 MN) hydraulic jack (Fig. 4(b)). The applied force was measured by a load cell placed between the hydraulic jack and the reaction steel frame. An assembly of steel plates and neoprene pads was placed on top of the column to uniformly spread the force over the entire column section. Initial loading increments of 20 kip (90 kN) were used until the load approached the predicted strength of the specimen. After each loading step, the applied load was held constant so the development of cracks in the slab could be recorded. Smaller load increments were then used to capture the peak load resisted by the specimen. When the specimen started to fail, the column was continuously pushed downward until the load decreased below 60% of the peak specimen strength. The total testing time for each specimen was approximately 45 minutes.

Measurement apparatus—Strains in slab reinforcement and shear studs were measured through 0.2 in. (5 mm) long electronic strain gauges at the locations shown in Fig. 3(c) and Fig. 1, respectively. Displacement of the slabs and columns was monitored using a three-dimensional (3-D) motion-tracking system. This system, which uses high-resolution infrared cameras, detects signals emitting from markers glued on the specimens (Fig. 4 and 5). Local x, y, and z coordinates of each marker were recorded at 10 Hz with an accuracy of 0.004 in. (0.1 mm). To monitor the development of inclined cracks and failure surfaces inside the slabs during the tests, through-thickness (vertical) expansion of the slab at various locations was measured by pairs of markers, as shown in Fig. 5. For each pair, one marker was glued on the top surface of the slab and the other was attached to the top of a threaded rod. The steel rod extended vertically through the slab inside a 1/4 in. (6 mm) diameter plastic pipe and the other end of the rod was attached to the bottom of the slab. A steel spring, preloaded in compression, was placed between the slab and the top of the threaded rod to stabilize the measurement unit. A relative displacement between the two markers indicated an expansion of the slab.

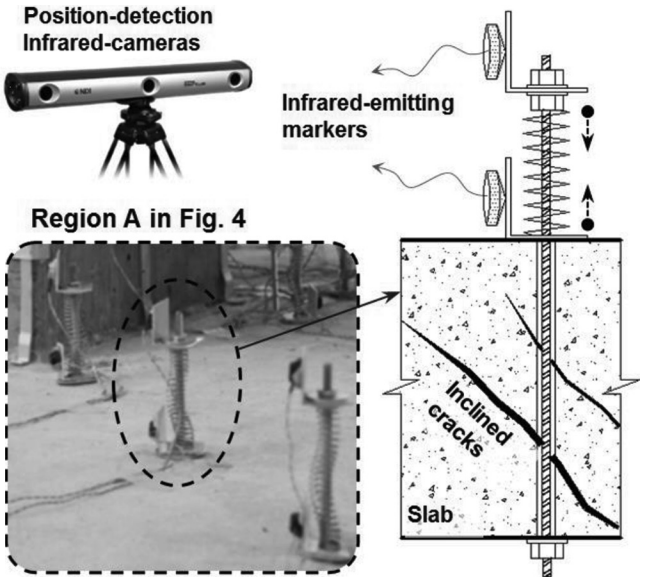

Fig. 5—Measurement of through-thickness expansion of slabs.

EXPERIMENTAL RESULTS

Overall behavior

All specimens were loaded until failure and the maximum applied load V_u for each specimen is given in Table 2. Control Specimen S08C, without shear reinforcement, experienced a typical punching shear failure at V_u = 233 kip (1040 kN), which corresponded to a stress $v = 4.2\sqrt{f_c'}$ psi ($0.35\sqrt{f_c'}$ MPa). The other specimens, with shear studs, also failed due to punching shear, but their measured strengths V_u were 25% to 35% higher than that of Specimen S08C. Thus, the shear studs increased the shear

Table 2—Specimen calculated strengths and test results

ID	V_u, kip (kN)	V_{shear}, kip (kN)	V_{flex}, kip (kN)	V_{shear}/V_{flex}	V_u/V_{shear}	V_u/V_{flex}	$v_u/\sqrt{f'_c}$, psi (MPa)	Failure mode
(1)	(2)	(3)	(4)	(5)	(6)	(7)	(8)	(9)
S08C	233 (1040)	222 (990)	285 (1270)	0.8	1.1	0.8	4.2 (0.35)	Punching shear
S08O	287 (1280)	317 (1410)	285 (1270)	1.1	0.9	1.0	5.67 (0.47)	Flexurally triggered punching shear
S08R	293 (1300)	322 (1430)	285 (1270)	1.1	0.9	1.0	5.62 (0.47)	Flexurally triggered punching shear
S12O	301 (1340)	304 (1350)	390 (1740)	0.8	1.0	0.8	6.44 (0.53)	Punching shear
S12R	314 (1400)	308 (1370)	390 (1740)	0.8	1.0	0.8	6.51 (0.54)	Punching shear

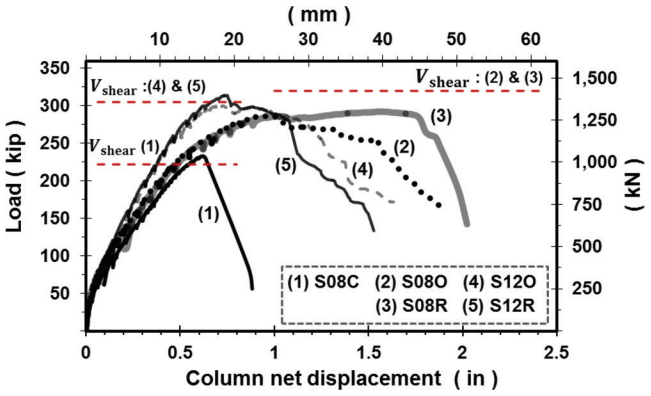

Fig. 6—Load versus displacement.

strength for all of the slab-column connections with shear reinforcement.

A ratio of the measured shear strength V_u for each specimen to the corresponding nominal shear strength V_{shear} calculated using the ACI Code,[13] is given in Column 6 of Table 2. It can be seen that $V_u/V_{shear} \geq 1$ for Specimen S08C and the S12 specimens, but $V_u/V_{shear} \cong 0.9$ for Specimens S08O and S08R. This means that the ACI Code[13] equations for shear strength of slab-column connections overestimated the strength of Specimens S08O and S08R, which had a lower slab flexural reinforcement ratio ρ.

Measured load versus column displacement relationships for all specimens are shown in Fig. 6. It can be seen that the S08 specimens (Lines 1, 2, and 3), with a lower ρ, had a lower post-cracking stiffness than the S12 specimens (Lines 4 and 5). Specimen S08C (Line 1) showed a sudden drop in load capacity at 233 kip (1040 kN) due to a punching shear failure. For the specimens with shear studs, the failure sequence started with a slight drop in load capacity at a column displacement of approximately 1 and 0.7 in. (25 and 18 mm) for the S08 and S12 specimens, respectively. After that, the behavior of the pairs of specimens in each group was different.

Specimens S08O and S08R—Figure 6 shows that Specimens S08O (Line 2) and S08R (Line 3) behaved similarly up to an applied load of approximately 290 kip (1290 kN), where both specimens suffered a slight drop in their load capacity. After this point, the behavior of Specimens S08O and S08R were significantly different. While the specimen with an orthogonal layout of shear studs, S08O, continuously lost strength (Line 2), Specimen S08R, with a radial layout of shear studs, recovered strength and exhibited a more ductile behavior (Line 3). These observations are similar to the test results reported by DaCosta and Parra-Montesinos,[11] and Broms.[10]

Specimens S12O and S12R— Figure 6 shows that Specimens S12O (Line 4) and S12R (Line 5) behaved similarly until the applied load reached approximately 80% of their maximum load capacities. Beyond that point and up to the peak load, Specimen S12R retained slightly more stiffness than Specimen S12O. The two specimens reached to their maximum load capacities at column displacement of approximately 0.7 in. (18 mm). After that, their load capacities both dropped continuously as the column displacement increased. The measured strength of Specimen S12R (radial layout) was 314 kip (1400 kN), which was similar ($\cong$ 5% higher) to that of Specimen S12O (orthogonal layout). This finding was similar to the test results reported by Birkle and Dilger.[7]

Although, in each pair, measured strengths for the two specimens with different layouts of shear studs were similar, the observed failure surface and measured strains in the shear studs for the specimens with an orthogonal layout of shear studs were very different from those for the specimens with a radial layout of shear studs. A description of these differences is presented in the following sections.

Flexural behavior

Flexural cracks—Flexural cracks observed on the tensile surface of the slabs consisted of circumferential (ring-shaped) and radial (fan-shaped) cracks. While the circumferential cracks formed around a column at various distances from the column faces, the latter developed radially (perpendicularly to the circumferential cracks) from the region close to the columns toward the edge of the slabs. The first circumferential crack occurred close to the column perimeter at an applied load of 30 to 40 kip (130 to 180 kN), and resulted in a softening of the load-versus-displacement relationship for all specimens (Fig. 6). The second and third circumferential cracks formed later and at distances of approximately 0.5*d* and 1.25*d* from the column faces as the applied load increased from 120 to 160 kip (530 to 710 kN) and 180 to 190 kip (800 to 850 kN), respectively. The radial cracks occurred after the first circumferential crack. These initiated in the region adjacent to the column faces when the applied load

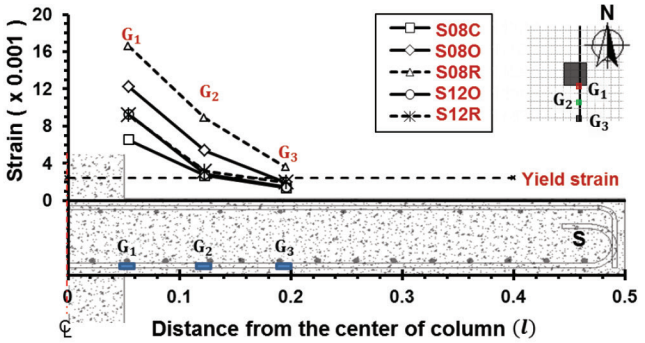

a) Gauges G1, G2, and G3

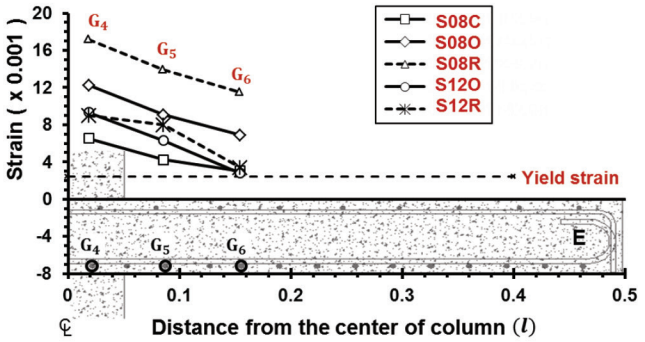

b) Gauges G4, G5, and G6

Fig. 7—Strain distribution in flexural reinforcement at maximum loads.

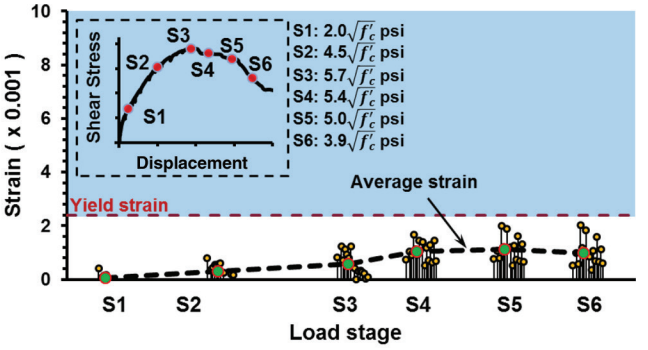

a) Specimen S08O (similar to S12O), orthogonal layout

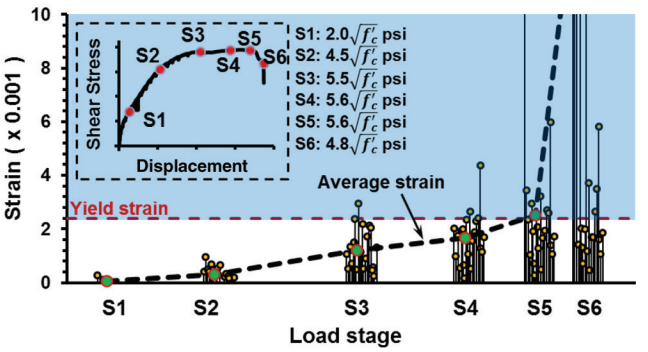

b) Specimen S08R (similar to S12R), radial layout

Fig. 8—Measured strains in shear studs.

reached approximately 70 kip (310 kN) for the S08 specimens and 90 kip (400 kN) for the S12 specimens. While the radial cracks propagated all the way to the edges of the slabs in Specimens S08O and S08R, they stopped at approximately 3*d* from the column faces in the S12 specimens.

Development of flexural yielding—Measured strain distributions in slab flexural reinforcement at the maximum load for all specimens are shown in Fig. 7. The spread of the flexural yielding away from the south face of the column for one north-south bar near the center of the slab (Gauges G1 to G3) is shown in Fig. 7(a). The measured strains indicate that plastic hinging regions in the test specimens extended approximately to 0.15*l* to 0.25*l* (*l* is the span length of specimens), or 2*d* to 3.5*d*, from the center of columns. Figure 7(b), Gauges G4 to G6, shows the spread of the flexural yielding away from the west face of the column for three north-south bars. It can be seen that slab flexural mechanisms were more fully developed in Specimen S08R than in the other test specimens, which contributed to the higher ductility observed for Specimen S08R.

For all specimens, flexural reinforcement adjacent to the columns yielded. The strains in the slab flexural reinforcement were smallest in Specimen S08C. The measured strains in slab flexural reinforcement in the S12 specimens were similar, but lower than the strains in the S08 shear-reinforced specimens, which had a lower slab reinforcement ratio. The measured strains for Specimen S08R were significantly higher than Specimen S08O, which corresponds to the more ductile behavior of Specimen S08R in Fig. 6.

It has been observed that yielding of slab flexural tension reinforcement near a column allows a wider opening of shear cracks close to the column, which reduces aggregate interlock along these cracks[1,16,17] Significant yielding of slab flexural reinforcement near the columns in Specimens S08O and S08R is believed to have been a primary cause for the lower shear strengths measured for those specimens, and their failure mode was thus called "flexurally triggered punching shear" in Table 2.

The load required to develop a flexural mechanism in the slabs (V_{flex}) for the test specimens, estimated by yield-line analysis,[18-20] is given in Eq. (2)

$$V_{flex} = \frac{4\sqrt{2}}{\cos\left(\frac{\pi}{8}\right) - \frac{h_c\sqrt{2}}{l}} m \quad (2)$$

in which h_c is the column side dimension; l is the specimen span length; and m is the slab moment strength per unit width given in Eq. (3).

$$m \cong \left(1 - \frac{\rho f_y}{1.7 f_c'}\right) \rho f_y d^2 \quad (3)$$

Calculated V_{flex} for each test specimen is given in Table 2. For the S12 specimens, V_{flex} was approximately 30% larger than the ACI Code nominal shear strength (V_{shear}); thus, V_{shear} governed the measured failure loads of these specimens. For Specimens S08O and S08R, however, V_{flex} was approximately 10% smaller than the corresponding calculated shear strength V_{shear}, and the measured loads at "flexur-

ally triggered punching shear failure" for Specimens S08O and S08R (Table 2) were close to V_{flex}.

Shear behavior

Strains in shear studs—Strains measured in the instrumented shear studs (Fig. 1) at six load stages, S1 to S6, during the tests of Specimen S08O (similar to S12O) and S08R (similar to S12R) are shown in Fig. 8(a) and 8(b), respectively. The dashed lines in Fig. 8 represent averages of the measured strains. It can be seen that the average strains for the two layouts of shear studs developed similarly until Stage S2 (measured $v = 4.5\sqrt{f_c'}$ psi [$0.37\sqrt{f_c'}$ MPa]). After that load stage, the strains in the shear studs in a radial layout increased at a higher rate. At Stage S3, when all of the specimens experienced a slight drop or leveling off in load capacity, strains in many of the shear studs in the radial layout reached or exceeded the yield strain (0.0024), but none of the shear studs in the specimens with an orthogonal layout of shear studs yielded. For the radial layout of shear studs, strains in shear studs increased rapidly beyond Stage S3 (Fig. 8(b)), especially for the shear studs closest to the column. Some shear studs close to the column fractured near load Stages S5 and S6. Strains in shear studs for the orthogonal layout, however, remained nearly constant and below the yield strain after load Stage S3 (Fig. 8(a)).

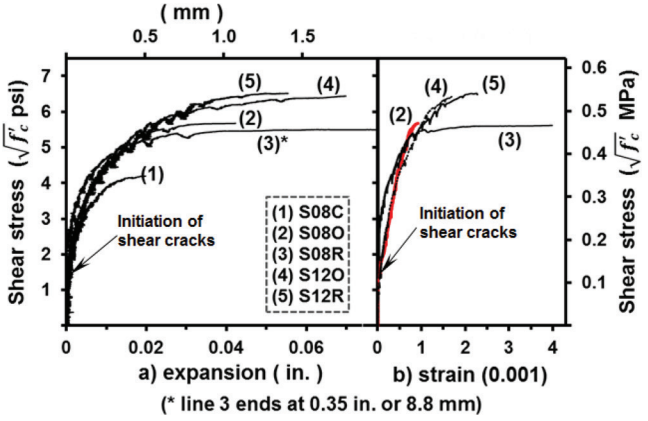

*Fig. 9—(a) Measured through-thickness slab expansions at approximately 0.5*d *from column faces; and (b) strains in the shear studs close to columns.*

These strain measurements indicate that the failure surfaces engaged the shear studs when arranged in a radial layout, but not when arranged in an orthogonal layout.

Shear cracks—It was not possible to observe shear (inclined) cracks during the tests because they developed inside the slabs. The development of inclined cracks, however, can be studied from the measured through-thickness expansion of the slabs (Fig. 9(a)) and strains in the shear studs (Fig. 9(b)). Based on the data in Fig. 9, shear cracks may have initiated when slab shear stresses reached approximately 1.5 $\sqrt{f_c'}$ psi ($0.125\sqrt{f_c'}$ MPa). Because the circumferential flexural cracks that could initiate flexural-shear cracking had not been observed at this loading stage, the formation of the inclined cracks in the slabs was assumed to be similar to that of web-shear cracks in beams. Thus, these inclined cracks were likely initiated near the middepth of the slabs and then extended toward the top and bottom of the slabs.

After the tests were completed, the specimens were cut along a line close to the north face of the columns to observe crack patterns in the slabs. The cut surfaces are shown in Fig. 10. Specimen S08C, without shear reinforcement, had a single shear crack, as seen in Fig. 10(a). For the other specimens, several inclined cracks can be observed within the regions reinforced with shear studs (Fig. 10(b) to 10(e)).

Splitting cracks—The cut surface for Specimen S08O (Fig. 10(b)) shows a horizontal splitting crack located above the shear studs. This horizontal splitting crack became an inclined crack beyond the outermost set of shear studs. A similar splitting crack can be seen in Specimen S12O (Fig. 10(d)). For Specimens S08R and S12R, with a radial layout of shear studs, horizontal splitting cracks appeared near the columns before joining with inclined cracks that extend through the second and third line of shear studs from the column (Fig. 10(c) and 10(e)).

The horizontal splitting cracks were not observed during the tests because the top of the slabs remained intact. The development of splitting cracks, however, can be studied from the measured strains in shear studs and through-thickness expansion of the slabs. Figure 9 shows that, for Specimen S08O (Lines 2), at the maximum load, measured strain in one of the innermost shear studs and the nearby through-thickness expansion of the slab were 0.92E-3 and 0.042 in. (1.1 mm), respectively. A calculated elongation of

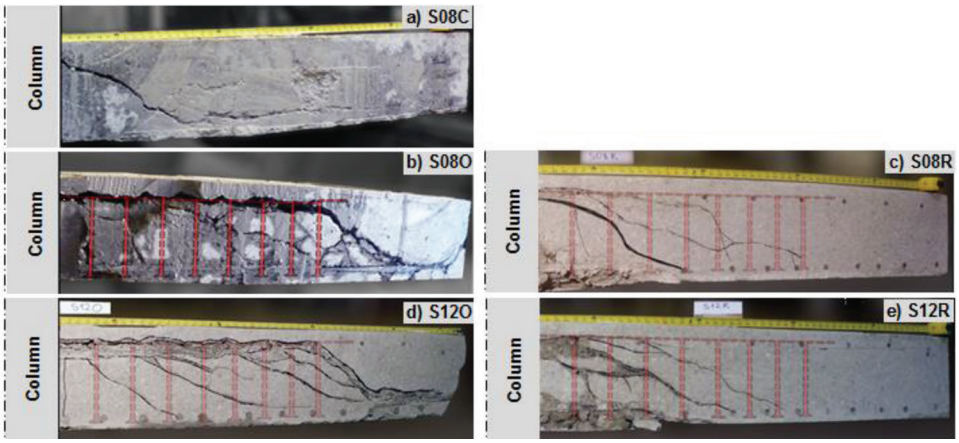

Fig. 10—Inclined cracks and failure surfaces on cut sections.

this stud, given its smooth shaft length of 8.5 in. (216 mm), was 0.008 in. (0.2 mm), which is approximately 20% of the measured expansion of the slab. Thus, approximately 80% of the slab expansion at this stage can be attributed to the horizontal splitting crack that formed above the shear studs. Similar results were obtained for Specimen S12O.

Failure behavior—Control Specimen S08C, without shear reinforcement, failed due to a typical punching shear failure (Line (1) in Fig. 6). For the other specimens with shear studs, the failure sequence started with a slight drop in load capacity (Lines (2) to (5) in Fig. 6) at a column displacement of approximately 1 and 0.7 in. (25.4 and 18 mm) for S08 and S12 specimens, respectively. The formation of the horizontal splitting cracks near the columns, as observed in Fig. 10, is assumed to have caused these drops in load capacity. This state can also be considered as an initiation of punching failure, as the column and adjacent slab displacements started to deviate. Beyond this stage, the development of the failure surfaces depended on the configuration of shear studs.

For Specimens S08O and S12O (orthogonal layout of shear studs), inclined cracks developed adjacent to the orthogonal stud rails and in the diagonal regions adjacent to the corners of the columns, shown as Cracks (3) in Fig. 11(a) and 11(b). These crack surfaces extended away from the column faces and remained parallel to the stud rails. These inclined cracks adjacent to the stud rails and the splitting cracks over the top of the studs created the failure surfaces that separated the shear studs from the slabs. It can be seen from Fig. 11(b) that the propagation of those failure surfaces (Cracks (3)) was not restrained because of the absence of shear reinforcement in the diagonal regions. Thus, these failure surfaces continuously extended away from the columns to the outermost shear studs, resulting in the nearly cruciform-shaped failure cones shown in Fig. 11(c). During this progress, shear studs were not engaged by the failure surfaces and the strain in the studs remained relatively low and constant up to failure (Fig. 8(a)). Extending the stud rails further away from the columns may not have improved the behavior and strength of these specimens.

For Specimens S08R and S12R (radial layout of shear studs), horizontal splitting cracks did develop above the stud rails in almost circular regions close to the column faces, but these cracks were not a significant part of the failure sequence for these specimens. The final failure in these specimens took place along a truncated-pyramid surface that engaged the shear studs near the columns. These shear studs developed their yield strength and, thus, supported the development of a flexural mechanism in the slabs, especially for Specimen S08R, which had a lower slab flexural reinforcement ratio and $V_{flex} < V_{shear}$.

COMPARISONS WITH PRIOR RESEARCH AND RECOMMENDATIONS

Test results from this study show that the conflicting results reported by previous research investigations[7,10,11] are likely related to the percentage of slab flexural reinforcement (ρ). Main specimen properties and test results from those research investigations[7,10,11] and this study are given in Table 3. The

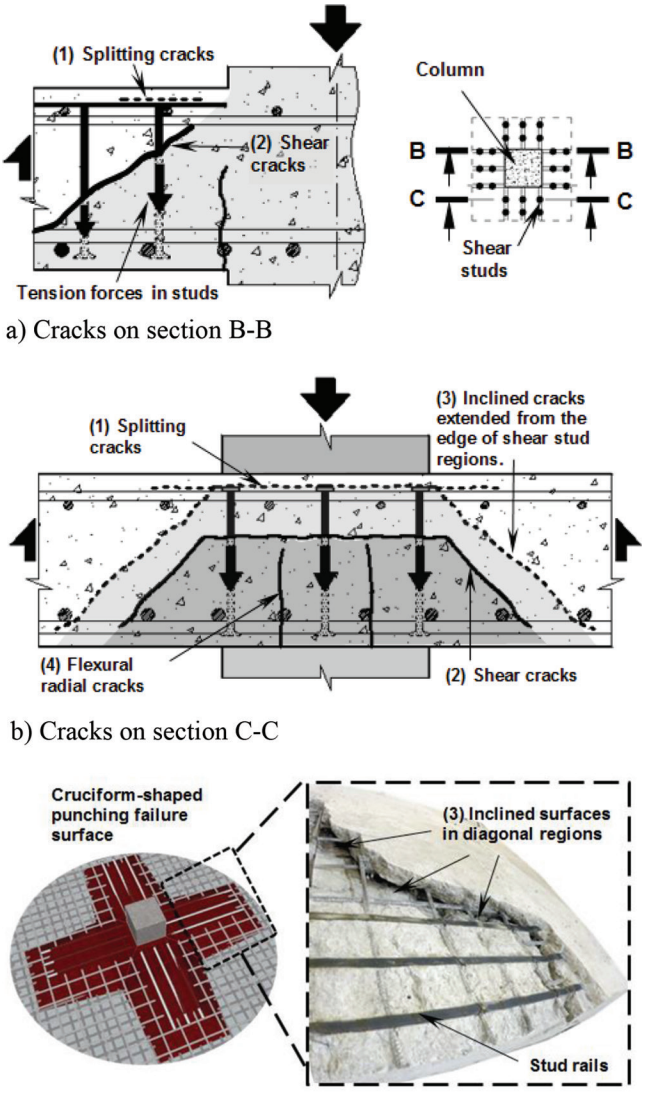

Fig. 11—Failure surfaces in specimens with orthogonal stud layout.

test specimens are divided into two groups based on the ratio of V_{flex}/V_{shear}, in which V_{flex} is the calculated flexural strength of the test specimens[21] based on a yield-line analysis in the region of the slab adjacent to the column, and V_{shear} is the calculated shear strength from Eq. (1). The first group has $V_{flex}/V_{shear} > 1$ (relatively high ρ), and the other group has $V_{flex}/V_{shear} \le 1$ (relatively low ρ). It was found that test results within each group are consistent. In the following sections, the effects of shear stud layout and slab flexural reinforcement ratio on the behavior and strength of slab-column connections in each of these groups are discussed.

Effect of shear stud layout

Punching shear strength—Table 3 shows that for the specimens with a relatively high ρ (Group 1), even though the failure pattern may be different, an orthogonal layout of shear studs provided the same shear strength as a radial layout. On the other hand, for the specimens with a relatively low ρ (Group 2), an orthogonal layout of shear studs might

Table 3—Results from studies of gravity-loaded slab-column connections reinforced with shear studs in radial or orthogonal layout

Study	ID	ρ, %	$\beta = b_c/L$	$\alpha = b_c/d$	Layout	V_{flex}/V_{shear}	V_u, kip	V_u/V_{shear}	V_u/V_{flex}	μ
(1)	(2)	(3)	(4)	(5)	(6)	(9)	(9)	(10)	(11)	(12)
Group 1: specimens with relatively high ρ ($V_{flex}/V_{shear} > 1$)										
Birkle[7]	S2	1.51	0.05	2.02	Ortho.	1.32	129	1.03	0.78	NA
	S3	1.51	0.05	2.02	Radial	1.32	129	1.01	0.77	2.1
	S5	1.51	0.05	2.02	Ortho.	1.19	140	1.01	0.85	2.5
	S6	1.51	0.05	2.02	Radial	1.22	138	1.02	0.84	2.5
Ferreira and Melo[9]	C4*	1.52	0.06	2.28	Ortho.	1.22	252	1.21	0.99	NA
	C8*	1.47	0.06	2.28	Radial	1.21	238	1.11	0.91	NA
This research	S12O	1.27	0.04	1.41	Ortho.	1.28	301	0.99	0.79	2.2
	S12R	1.27	0.04	1.41	Radial	1.27	314	1.02	0.82	2.2
	S08C	0.87	0.04	1.39	—	1.27	233	1.05	0.82	1.3
Group 2: specimens with relatively low ρ ($V_{flex}/V_{shear} \le 1$)										
Broms[10]	18a	1.29	0.05	2.16	Ortho.	0.93	193	0.84	0.90	2.4
	18b*	1.21	0.05	2.16	Radial	0.92	218	0.87	0.95	3.4
This research	S08O	0.87	0.04	1.39	Ortho.	0.90	287	0.92	1.01	2.8
	S08R	0.87	0.04	1.39	Radial	0.89	293	0.91	1.02	3.6
DaCosta and Parra-Montesinos[11]	M1	0.77	0.03	0.92	Ortho.	0.61	134	0.59	0.96	1.5
	M9	0.80	0.03	0.96	Radial	0.75	136	0.75	1.00	4.1

*Stud spacing was larger than limits specified in ACI Code.[13]

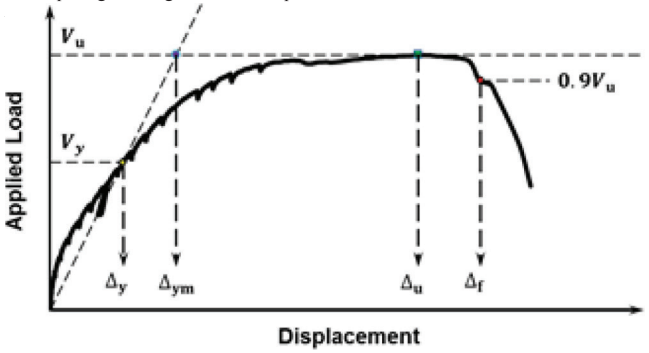

Fig. 12—Definition of ductility.

provide a lower shear strength than a radial layout. The study by Broms[10] showed that load capacity of Specimen 18b, with a radial layout of shear studs, was 13% higher than that of Specimen 18a, reinforced with shear studs in an orthogonal layout.

Specimen ductility—Results from recent investigations[10,11,19] indicate that a radial layout of shear studs led to more ductile behavior than an orthogonal layout. To make a quantifiable comparison, displacement ductility μ was used as given by Eq. (4)

$$\mu = \Delta_f/\Delta_{ym} \quad (4)$$

where Δ_f is the displacement when the applied load decreases to 90 percent of the maximum load V_u; and Δ_{ym} is the displacement at the intersection point between the horizontal line corresponding to the maximum load V_u and a secant line from the origin through the point corresponding to an initial yielding of the flexural reinforcement (Δ_y, V_y), as illustrated in Fig. 12. An approximation $V_y \cong 2/3V_u$ was used[22,23] for tests in which information of an initial yielding point was not reported.

Calculated ductility μ for all specimens is given in Column 12 of Table 3. It can be seen that for Group 2 (relatively low ρ), the calculated ductility for specimens with a radial layout of shear studs was higher than that for the corresponding specimens with an orthogonal layout in the same study. Also, the calculated ductility provided by a radial layout increased when the relative slab flexural reinforcement ratio V_{flex}/V_{shear} decreased. For specimens with an orthogonal layout, however, no improvement was found in the calculated ductility as the ratio V_{flex}/V_{shear} decreased.

Effect of percentage of slab flexural reinforcement ρ

It can be seen from Table 3 that, for the specimens in Group 1, the measured load capacities were close to the corresponding shear strength calculated using the ACI Code.[13] However, for the specimens in Group 2, the

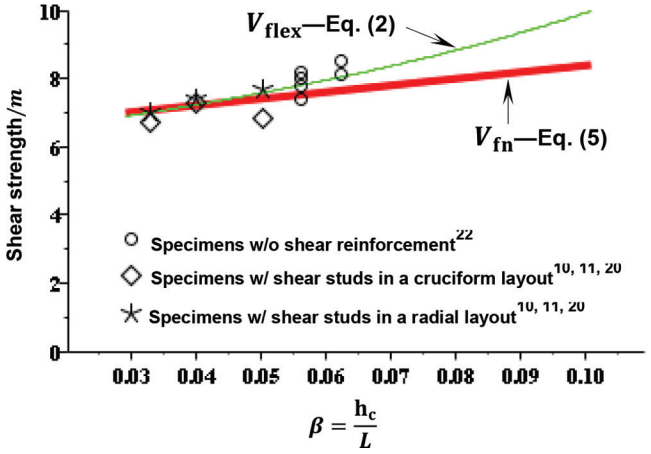

Fig. 13—Punching failure loads for specimens with relatively low ρ.

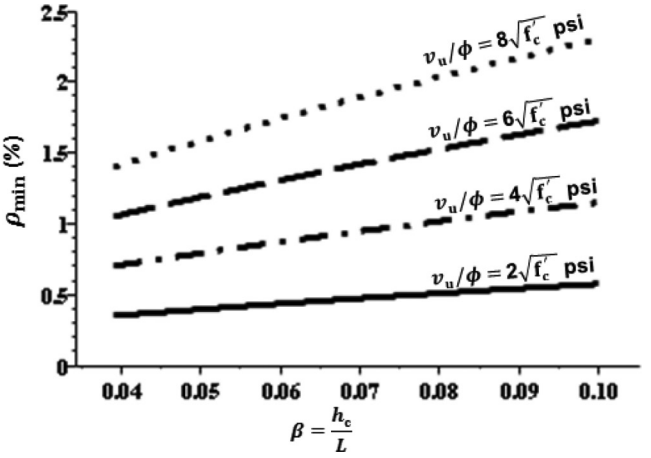

Fig. 14—Minimum of slab flexural reinforcement ρ. (Note: $1\sqrt{f_c'}$ psi $=0.083\sqrt{f_c'}$ MPa.)

measured loads at punching shear failure were substantially lower than the corresponding ACI Code calculated shear strengths (Column 10). Similar observations have also been reported[16,21,24-26] for specimens without shear reinforcement and with a low ρ. Thus, the ACI Code provisions for punching shear strength may be unconservative for slab-column connections with a low percentage of slab flexural reinforcement. To determine the lower-bound shear strength of a slab-column connection, design procedures should include an evaluation of the gravity shear required to develop a flexural mechanism that involves slab flexural yielding around the column. This will be referred to as local flexurally induced shear strength (V_{fn}).

The calculation of V_{fn} in an actual structure needs to at least consider: 1) application of uniform loads on the slab; and 2) the shift of contraflexural lines as plastic deformations take place. Considering these aspects, the authors have derived (refer to the Appendix*) a simple expression (Eq. (5)) to calculate V_{fn} at interior slab-column connections with negligible moment transfer, equal spans in both principal directions, and circular, square, or nearly square columns. A similar procedure may be applied to determine V_{fn} for other design scenarios.

$$V_{fn} \cong (6.5 + 20\beta)m \tag{5}$$

The expression for V_{fn} depends on the slab moment strength per unit width, m, and a parameter β defined as $\sqrt{A_c}/L$, in which A_c is the column cross-sectional area, and L is the slab span length. For square columns with side dimension h_c, $\beta = h_c/L$, which represents the column side dimension as a fraction of the span length.

Punching failure loads, expressed in terms of slab unit moment strength m for the specimens in Group 2 of Table 3 and other specimens[21] without shear reinforcement, but with a low ρ, are plotted in Fig. 13. These experimental results indicate that the measured shear strength of these specimens increased as β increased. The calculated flexural strength of the test specimens (V_{flex}) using Eq. (2), assuming $l = 0.4L$, and the proposed V_{fn} values from Eq. (5) are also plotted in Fig. 13. It can be seen that $V_{flex} = V_{fn}$ if the column dimension is less than 5% of the slab span ($\beta < 0.05$), but V_{flex} is significantly higher than the proposed V_{fn} when the column size to span length ratio increases. This difference is partially due to the assumed location of the contra-flexural lines ($l = 0.4L$), which becomes less accurate as β increases. In practice, β typically ranges from 0.04 to 0.1.

Proposed minimum slab flexural reinforcement—It has been shown[1,16,17] that yielding of slab flexural reinforcement near the columns may substantially reduce the shear capacity of slab-column connections, and thus, the maximum transferred shear force is likely limited by the local flexurally induced shear strength (V_{fn}). Thus, it is recommended that slab flexural reinforcement within the transfer width, which in the ACI Building Code is assumed to extend $1.5h$ (h is slab thickness) on each side of the column, be designed such that the corresponding V_{fn} is larger than the factored shear force V_u at the connection. Using V_{fn} given in Eq. (5), the required unit moment strength m of the slab within the transfer width is given in Eq. (6), where V_{fn} is taken equal to V_u/ϕ. The strength reduction factor ϕ should be the value used for shear design (0.75). The unit moment strength of a slab (m) is a function of ρ, as given in Eq. (3), and it can be approximated as $m \cong 0.9\rho f_y d^2$. Using this approximation, Eq. (6) gives a minimum value (ρ_{min}) for the slab flexural reinforcement ratio in the transfer width.

$$m \geq \frac{V_u/\phi}{6.5 + 20\beta} \tag{6}$$

$$\rho_{min} = \frac{V_u/\phi}{(5.85 + 18\beta) f_y d^2} \tag{7}$$

Assuming $f_y = 60{,}000$ psi, $f_c' = 5000$ psi, and $d \cong 0.9(L/33)$, the proposed ρ_{min} for interior slab-column connections with square columns transferring different levels of concentric slab shear stress ($v_u = V_u/b_o d$) is shown in Fig. 14. These

*The Appendix is available at **www.concrete.org/publications** in PDF format, appended to the online version of the published paper. It is also available in hard copy from ACI headquarters for a fee equal to the cost of reproduction plus handling at the time of the request.

results indicate that ρ_{min} increases as either the design shear stress or the column size-to-span length ratio β increases.

For the five test specimens presented herein, the ratio β was approximately 0.04. It can be seen from Fig. 14 that if the design slab shear stress for these specimens is $6\sqrt{f_c'}$ psi ($0.5\sqrt{f_c'}$ MPa), the minimum slab flexural reinforcement $\rho_{min} \cong 1.1\%$. Because the S08 specimens in this test series had $\rho_{min} \cong 0.9\%$, the maximum slab shear stresses transferred in Specimens S08O and S08R did not reach $6\sqrt{f_c'}$ psi (refer to Table 2). For the S12 specimens, however, which had ρ = 1.25%, the maximum measured slab shear stresses for these specimens were above of $6\sqrt{f_c'}$ psi. Figure 14 also shows that for specimens without shear reinforcement ($v_u/\phi = 4\sqrt{f_c'}$ psi [$0.33\sqrt{f_c'}$ MPa]), the minimum slab flexural reinforcement ratio should be approximately 1% for slab-column connections with a typical value of β (0.04 to 0.1), which is similar to suggestions from other studies.[26,27]

CONCLUSIONS

The following conclusions were drawn based on the results from the tests presented herein and other reported tests[10,11,25,28] of interior slab-column connections under monotonically increased loading, in which the slab thickness varied from 6 to 10 in. (150 to 250 mm). The symbol ρ in the conclusions represents the percentage of slab flexural tension reinforcement.

1. An orthogonal layout of shear studs provided similar strength as a radial layout for slab-column connections with sufficient flexural reinforcement such that a punching failure developed prior to the formation of a flexural mechanism.

2. A radial layout of shear studs led to a higher shear strength than an orthogonal layout for slab-column connections that exhibited slab flexural yielding prior to punching.

3. The observed failure surfaces engaged shear studs when arranged in a radial layout, but did not engage shear studs when used in an orthogonal layout. Thus, a radial layout of shear studs permitted the development of a full flexural mechanism in the test specimens with a 0.87% reinforcement ratio, which led to substantially greater ductility. A radial layout of shear studs is thus recommended, especially in the locations where ductility is important (for example, where redistribution of moments is accounted for in design).

4. The ACI Building Code nominal strength equations for punching shear at slab-column connections may overestimate shear strength for interior slab-column connections with low flexural tension reinforcement ratios. The gravity shear required to develop the slab flexural strength in the region around the column should be considered when evaluating the shear strength of slab-column connections.

5. For slab-column connections with circular, square, or nearly square columns that are part of a floor system with equal span lengths, the flexural tension reinforcement ratio within a slab transfer width that extends $1.5h$ (h is the thickness of slabs) on each side of the column should be greater than or equal to the proposed ρ_{min} given in Eq. (7).

AUTHOR BIOS

Thai X. Dam *is a PhD candidate in the Civil and Environmental Engineering Department at the University of Michigan, Ann Arbor, MI. His research interests include the behavior and design of reinforced concrete, and rehabilitation of existing reinforced concrete structures.*

James K. Wight, *FACI, is the Frank E. Richart Jr. Collegiate Professor of Civil Engineering at the University of Michigan. He is past Chair of ACI Committee 318, Structural Concrete Building Code, and Joint ACI-ASCE Committee 352, Joints and Connections in Monolithic Concrete Structures. His research interests include the behavior of reinforced concrete members and connections, hybrid steel-concrete structures, fiber-reinforced cementitious composites, and the seismic retrofit of existing structures.*

Gustavo J. Parra-Montesinos, *FACI, is the C.K. Wang Professor of Structural Engineering at the University of Wisconsin-Madison, Madison, WI. He is member of ACI Committee 318, Structural Concrete Building Code, and Chair of ACI Subcommittee 318-J, Joint and Connections. He is also member of Joint ACI-ASCE Committees 335, Composite and Hybrid Structures, and 352, Joints and Connections in Monolithic Concrete Structures. His research interests include the behavior and design of reinforced concrete, fiber-reinforced concrete, and hybrid steel-concrete structures.*

ACKNOWLEDGMENTS

This research was financially supported by the University of Michigan and Vietnam Education Foundation. The authors also would like to thank N. Hammill at Decon USA for his donation of the shear studs used in the project. The opinions presented in this paper are those of the authors and do not necessarily express the views of the sponsors.

REFERENCES

1. Joint ACI-ASCE Committee 426, "The Shear Strength of Reinforced Concrete Members—Slabs," *Journal of the Structural Division*, ASCE, V. 100, No. ST8, 1974, 50 pp.

2. CEB-FIB Bulletin 12, "Punching of Structural Concrete Slabs," Fédération internationale du béton, 2001, 308 pp.

3. Polak, M. A., ed., *Punching Shear in Reinforced Concrete Slabs*, SP-232, American Concrete Institute, Farmington Hills, MI, 2005, 302 pp.

4. Langohr, P. H.; Ghali, A.; and Dilger, W. H., "Special Shear Reinforcement for Concrete Flat Plates," *ACI Journal Proceedings*, V. 73, No. 3, Mar. 1976, pp. 141-146.

5. Mokhtar, A. S.; Ghali, A.; and Dilger, W., "Stud Shear Reinforcement for Flat Concrete Plates," *ACI Journal Proceedings*, V. 82, No. 5, Sept.-Oct. 1985, pp. 676-683.

6. Seible, F.; Ghali, A.; and Dilger, W. H., "Preassembled Shear Reinforcing Units for Flat Plates," *ACI Journal Proceedings*, V. 77, No. 1, Jan.-Feb. 1980, pp. 28-35.

7. Birkle, G., and Dilger, W., "Shear Strength of Slabs with Double-Headed Shear Studs in Radial and Orthogonal Layouts," *Thomas T. C. Hsu Symposium: Shear and Torsion in Concrete Structures*, SP-265, A. Belarbi, Y. L. Mo, and A. Ayoub, eds., American Concrete Institute, Farmington Hills, MI, 2009, pp. 499-510.

8. Dilger, W., "Flat Slab-Column Connections," *Progress in Structural Engineering and Materials*, V. 2, No. 3, 2000, pp. 386-399. doi: 10.1002/1528-2716(200007/09)2:3<386::AID-PSE43>3.0.CO;2-M

9. Ferreira, M. P.; Melo, G. S.; Regan, P. E.; and Vollum, R. L., "Punching of Reinforced Concrete Flat Slabs with Double-Headed Shear Reinforcement," *ACI Structural Journal*, V. 111, No. 2, Mar.-Apr. 2014, pp. 363-374.

10. Broms, C. E., "Ductility of Flat Plates: Comparison of Shear Reinforcement Systems," *ACI Structural Journal*, V. 104, No. 6, Nov.-Dec. 2007, pp. 703-711.

11. Post, N. M., "Tests Show Premature Failure of Shear-Stud Reinforcement," *Engineering News-Record*, Aug. 2011, p. 29.

12. Gomes, R., and Regan, P., "Punching Strength of Slabs Reinforced for Shear with Offcuts of Rolled Steel I-Section Beams," *Magazine of Concrete Research*, V. 51, No. 2, 1999, pp. 121-129. doi: 10.1680/macr.1999.51.2.121

13. ACI Committee 318, "Building Code Requirements for Structural Concrete (ACI 318-14) and Commentary (ACI 318R-14)," American Concrete Institute, Farmington Hills, MI, 2014, 519 pp.

14. Decon USA, "North American Manufacturer of Studrails®," Sonoma, CA.

15. ASTM A1044/A1044M-05(2010), "Standard Specification for Steel Stud Assemblies for Shear Reinforcement of Concrete," ASTM International, West Conshohocken, PA, 2010, 5 pp.

16. Hawkins, N.; Criswell, M.; and Roll, F., "Shear Strength of Slabs without Shear Reinforcement," *Shear in Reinforced Concrete*, SP-42, American Concrete Institute, Farmington Hills, MI, 1974, pp. 677-720.

17. Kinnunen, S., and Nylander, H., "Punching of Concrete Slabs without Shear Reinforcement," *Meddelande* No. 38, Institution for Byggnadsstatik, Kungliga Tekniska Högskolan, Stockholm, Sweden, 1960, 112 pp.

18. Wight, J. K., *Reinforced Concrete: Mechanics and Design*, seventh edition, Prentice Hall, 2015, 1168 pp.

19. Dam, T. X., and Wight, J. K., "Flexurally-Triggered Punching Shear Failure of Reinforced Concrete Slab-Column Connections Reinforced with Headed Shear Studs Arranged in Orthogonal and Radial Layout," *Engineering Structures*, V. 110, 2016, pp. 258-268. doi: 10.1016/j.engstruct.2015.11.050

20. Johansen, K. W., "Yield-Line Theory," Cement and Concrete Association, 1962, 181 pp.

21. Peiris, C., and Ghali, A., "Flexural Reinforcement Essential for Punching Shear Resistance of Slabs," *Recent Development in Reinforced Concrete Slab Analysis, Design, and Serviceability*, SP-287, M. Mahamid and F. Malhas, eds., American Concrete Institute, Farmington Hills, MI, 2012, 16 pp. (CD-ROM)

22. Stein, T.; Ghali, A.; and Dilger, W., "Distinction between Punching and Flexural Failure Modes of Flat Plates," *ACI Structural Journal*, V. 104, No. 3, May-June 2007, pp. 357-365.

23. Pan, A., and Moehle, J. P., "Lateral Displacement Ductility of Reinforced Concrete Flat Plates," *ACI Structural Journal*, V. 86, No. 3, May-June 1989, pp. 250-258.

24. Widianto; Bayrak, O.; and Jirsa, J. O., "Two-Way Shear Strength of Slab-Column Connections: Reexamination of ACI 318 Provisions," *ACI Structural Journal*, V. 106, No. 2, Mar.-Apr. 2009, pp. 160-170.

25. Guandalini, S.; Burdet, O. L.; and Muttoni, A., "Punching Tests of Slabs with Low Reinforcement Ratios," *ACI Structural Journal*, V. 106, No. 1, Jan.-Feb. 2009, pp. 87-95.

26. Ospina, C. E.; Birkle, G.; and Widianto, "Databank of Concentric Punching Shear Tests of Two-Way Concrete Slabs without Shear Reinforcement at Interior Supports," Structures Congress, 2012, pp. 1814-1832. doi: 10.1061/9780784412367.16010.1061/9780784412367.160

27. Joint ACI-ASCE Committee 421, "Guide to Design of Reinforced Two-Way Slab Systems (ACI 421.3R-15)," American Concrete Institute, Farmington Hills, MI, 2015, 28 pp.

28. Birkle, G., "Punching of Flat Slabs: The Influence of Slab Thickness and Stud Layout," PhD thesis, Department of Civil Engineering, University of Calgary, Calgary, AB, Canada, 2004, 235 pp.

APPENDIX—Evaluation of V_{fn}

*C*onsider a multi-span flat plate system supporting a uniform gravity load q on all panels. If the columns in the system have a circular section with a diameter D and are spaced equally at a distance L in orthogonal directions, the line of contra-flexure (zero radial bending moment) around an interior column is approximately a circle with diameter γL (Fig. A1a). Shear force transferred from the slab to the column is

$$V \cong q\left(L^2 - \frac{\pi D^2}{4}\right) \tag{A1}$$

The free-body diagram of an interior slab-column connection isolated from the floor system by the contra-flexure line is shown in Fig. A1 (b). For no moment transfer, it is reasonable to assume that a vertical shear ($R/\pi\gamma L$) is distributed uniformly along the perimeter of the slab. The total shear force acting along the edge of the slab (R) can be calculated from the equilibrium in the vertical direction and is given in Eq. (A2).

$$R = q\left(L^2 - \frac{\pi(\gamma L)^2}{4}\right) \tag{A2}$$

As the load q increases, yielding of slab flexural reinforcement initiates near the column faces and then spreads away from the column. Yield line analysis[19-21] will be used to evaluate shear force transfer at the connection (V_{fn}), assuming that a punching shear failure will occur after yielding of slab flexural reinforcement adjacent to the column, but prior to the formation of positive moment yield lines. Thus, the yield line analysis presented herein only involves circumferential and radial negative yield lines, as shown in Fig. A1 (b). Applying a virtual displacement δ at the edge of the slab, the external (EW) and internal work (IW) are given as,

$$\text{EW} \cong q\frac{2}{3}\left[\frac{\pi(\gamma L)^2}{4} - \frac{\pi D^2}{4}\right]\delta + R\delta \tag{A3}$$

$$\mathrm{IW} = m\pi(\gamma L)\frac{2\delta}{\gamma L - D} \tag{A4}$$

where m is moment strength of the slab per unit width. Combining Eq. (A2) through Eq. (A4) and setting $V = V_{\mathrm{fn}}$ in Eq. (A1) leads to,

$$V_{\mathrm{fn}} = 12m\frac{\pi\gamma\left[1-\left(\frac{\pi D^2}{4L^2}\right)\right]}{\left[\gamma/2-\left(\frac{\sqrt{\pi}D}{2L}\right)/\sqrt{\pi}\right]\left[12-8\left(\frac{\pi D^2}{4L^2}\right)-\pi\gamma^2\right]} \tag{A5}$$

where γ represents the location of the line of zero radial moment as a fraction of the span length L. Defining a parameter $\beta = \sqrt{A_{\mathrm{c}}}/L$, where A_{c} is the column cross sectional area, V_{fn} for the case of circular columns can be expressed as,

$$V_{\mathrm{fn}} = 12m\frac{\pi\gamma(1-\beta^2)}{(\gamma/2-\beta/\sqrt{\pi})(12-8\beta^2-\pi\gamma^2)} \tag{A6}$$

For slab-column connections with noncircular column cross sections, V_{fn} may be estimated from Eq. (A6) by taking $\beta = \frac{\sqrt{A_{\mathrm{c}}}}{L}$. Thus, for slab-column connections with square columns of side dimension h_{c} , $\beta = h_{\mathrm{c}}/L$.

To account for the shifting of the contra-flexure line as slab flexural yielding develops around the column faces, γ is assumed[19] to vary between 0.4 and 0.6. The ratio β is assumed to vary from 0.03 to 0.1. The relationship between V_{fn} and the parameters γ and β is shown in Fig. *A2* (a). It can be seen that V_{fn} increases as γ or β increases. From Fig. *A2* (b), which shows the relationships between V_{fn} and β for $\gamma = 0.4$, 0.5, and 0.6, it can be seen that a shift of the contra-flexure line has little effect on V_{fn} for β between 0.05 and approximately 0.07. As β approaches 0.1, however, V_{fn} decreases significantly as the contra-flexure line shifts away from the column. The following linear expression [Eq. (5) in main body of paper], plotted in

Fig. *A2* (b), represents a lower bound of V_{fn} for a typical value of β between 0.04 and 0.1 and γ between 0.4 and 0.6.

$$V_{\text{fn}} \cong (6.5 + 20\beta)m \tag{A7}$$

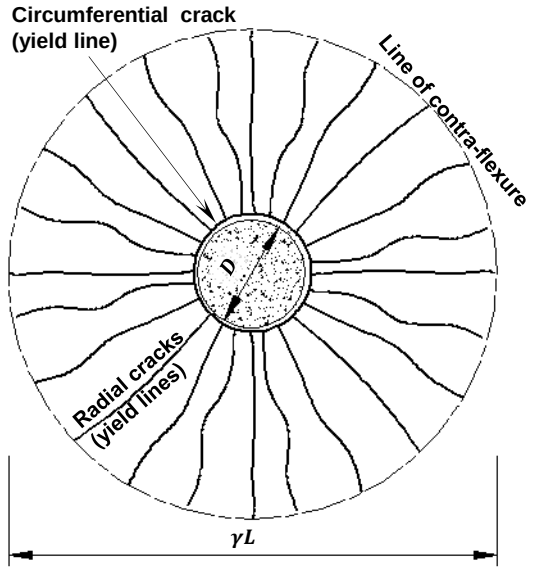

a) Top view

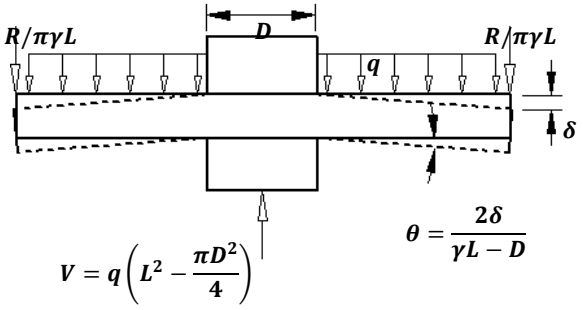

b) Free-body diagram and a virtual displacement

Fig. A1—Interior slab-column connection

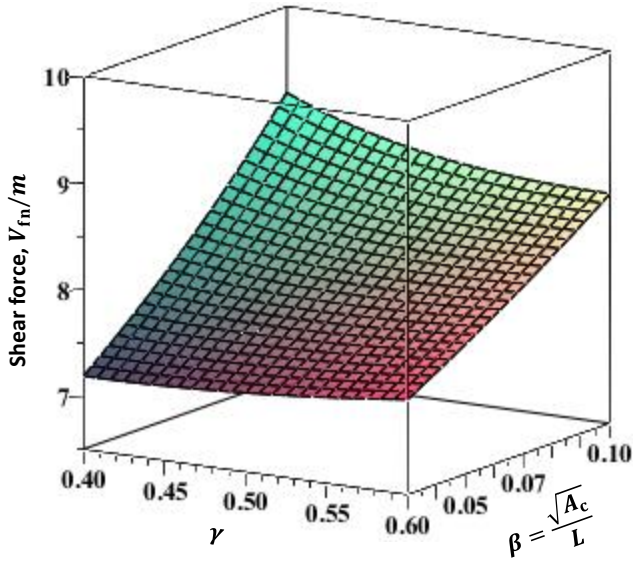

a) 3D plot of V_{fn} as given in Eq. (A6)

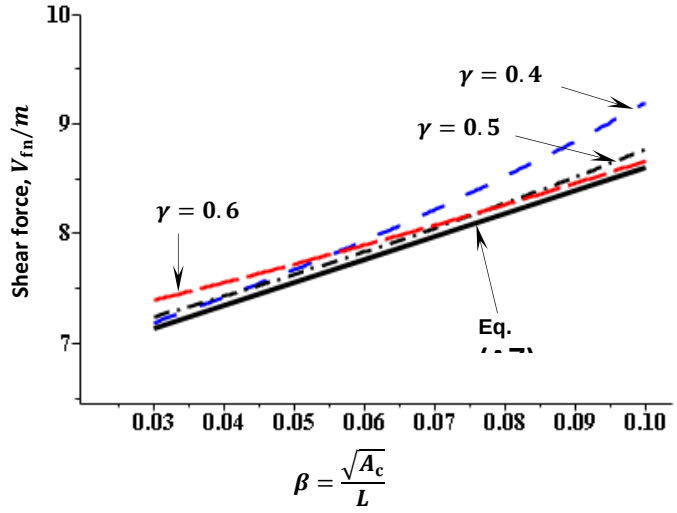

b) Comparison of V_{fn} given in Eq. (A6) at selected γ-planes and Eq. (A7)

Fig. A2—Shear force transferred at the connection